

ORIGINAL ARTICLE

Rapid shifts in picoeukaryote community structure in response to ocean acidification

Nicholas G Meakin and Michael Wyman

School of Biological and Environmental Sciences, University of Stirling, Stirling, UK

Rapid shifts in picoeukaryote community structure were observed during a CO₂ perturbation experiment in which we followed the development of phytoplankton blooms in nutrient-amended mesocosms under the present day or predicted future atmospheric pCO₂ (750 μatm, seawater pH 7.8). Analysis of *rbcL* clone libraries (encoding the large subunit of RubisCO) and specific quantitative PCR assays showed that two prasinophytes closely related to *Micromonas pusilla* and *Bathycoccus prasinus* were present, but responded very differently to high CO₂/acidification. We found that the abundance of *Micromonas*-like phylotypes was significantly higher (>20-fold) under elevated CO₂/low pH, whereas the *Bathycoccus*-like phylotypes were more evenly distributed between treatments and dominated the prasinophyte community under ambient conditions.

The ISME Journal (2011) 5, 1397–1405; doi:10.1038/ismej.2011.18; published online 17 March 2011

Subject Category: microbial population and community ecology

Keywords: picoeukaryotes; ocean acidification; *Micromonas*; *Bathycoccus*; RubisCO

Introduction

Approximately one-third of the carbon dioxide released to the atmosphere due to human activities, such as the combustion of fossil fuels, cement production and deforestation has been taken up by the oceans (Doney *et al.*, 2009). Uptake of anthropogenic CO₂ causes shifts in the marine carbonate system, which has led to a decline in seawater pH from a mean of 8.21 in preindustrial times to a present value of 8.1 (The Royal Society, 2005). Assuming little change in the prevailing trend in emissions, atmospheric CO₂ concentrations are predicted to increase from ~390 ppmV at present (compared with ~280 ppmV, 200 years ago) to 750–800 ppmV by the end of the current century, resulting in a further decline in seawater pH of 0.3–0.4 units (The Royal Society, 2005).

Acidification shifts chemical speciation within the oceans, resulting in an overall reduction in carbonate ion (CO₃²⁻) concentrations, with corresponding increases in bicarbonate (HCO₃⁻) and CO_{2(aq)} (Caldiera and Wickett, 2003). In comparison with preindustrial times, hydrogen ion concentrations are now ~30% higher in the upper ocean, whereas CO₃²⁻ concentrations are ~16% lower (Guinotte and Fabry, 2008). By the end of this century, CO₃²⁻ concentrations will decline further by

~40%, leading to an overall reduction in CO₃²⁻ to about half that of the surface oceans in the early nineteenth century. This will result in a significant reduction in the calcium carbonate saturation state, with potentially major impacts on both calcifying and non-calcifying marine organisms (Fabry *et al.*, 2008). The chemical speciation of many other elements, including those such as nitrogen (ammonia), phosphorus and iron that are required to support primary production, is also influenced by acidification, although the possible effects on marine ecosystems of these shifts in speciation largely remain to be assessed (Doney *et al.*, 2009; Breitbarth *et al.*, 2010).

Primary production within the oceans is dominated by the picoplanktonic size fraction (<2–3 μm cell diameter), which is composed of members of the cyanobacterial genera *Prochlorococcus* and *Synechococcus* and small unicellular photosynthetic algae, known collectively as picoeukaryotes (Stockner, 1988). Although picoeukaryotes are generally less abundant, their overall contribution to picoplankton biomass and annual production may well exceed that of cyanobacteria (Li, 1994; Worden *et al.*, 2004). The taxonomic diversity of picoeukaryotes is high (Moon-van der Staay *et al.*, 2001) and they include representatives from at least nine algal classes (Not *et al.*, 2004; Vaultot *et al.*, 2008). Members of the Prasinophyceae appear to be the most abundant picoeukaryotes in coastal waters, however, and three genera (*Micromonas*, *Bathycoccus*, *Ostreococcus*) belonging to the order Mamiellales have been commonly recorded (Not *et al.*, 2004; Zhu *et al.*, 2005; Marie *et al.*, 2006;

Correspondence: Dr M Wyman, School of Biological and Environmental Sciences, University of Stirling, Cottrell Building, Stirling, FK9 4LA, UK.

E-mail: michael.wyman@stir.ac.uk

Received 26 August 2010; revised 20 January 2011; accepted 22 January 2011; published online 17 March 2011

Worden, 2006). *Micromonas*, in particular, is thought to be of ubiquitous distribution in the world ocean (Slapeta *et al.*, 2006), and it has been proposed as a sentinel organism for monitoring the impact of climate change on marine ecosystems and biogeochemical cycles (Worden *et al.*, 2009).

We participated in a CO₂ perturbation experiment in which we investigated the effects of seawater acidification on phytoplankton diversity in mesocosms representing pCO₂ and pH predicted for the end of the century (750 µatm CO₂, pH 7.8) in comparison with that in present-day controls (~300 µatm CO₂, pH 8.1). Following nutrient (N, P) additions to stimulate growth, phytoplankton blooms developing within the mesocosms were sampled daily and their taxonomic diversity was investigated through sequence analysis of *rbcL* (encoding the large subunit of carbon-fixing enzyme, ribulose biphosphate carboxylase/oxygenase, RubisCO) clone libraries. In this paper, we report on the temporal dynamics of two prominent *rbcL* phylotypes recovered from the mesocosms, that we refer to as *Micromonas*-like and *Bathycoccus*-like, because of their high identity to published sequences from these two prasinophyte genera.

Materials and methods

Experimental background and sampling

Observations were made within an embayment of the Raunefjorden at the large-scale mesocosm facility at the University of Bergen Espegrend field station (60° 16' 10" N, 5° 13' 20" E). Full details of the setup and management of the mesocosms during this experiment are provided by Hopkins *et al.* (2010). Briefly, six clear polyethylene enclosures (2 m diameter, 3.5 m deep) located 200 m offshore were filled with unfiltered seawater (~11 m³; 31.4 psu), pumped from a depth of 1 m below the pontoon supporting the enclosures. The mesocosms were covered with high UV-transmitting horticultural polyethylene (photosynthetically active radiation transmission 92%) and three of the enclosures (1–3) were bubbled gently with air enriched to 750 ppmV CO_{2(g)} for two days, until the pH of the seawater within the enclosures had declined to ~7.8 (range 7.81–7.82). The remaining three mesocosms (4–6) were bubbled with air for the same period (to control for any effects of bubbling) and pH values at the beginning of biological sampling were within the range 8.14–8.15 (Hopkins *et al.*, 2010).

Biological sampling was initiated the next day (day 0), following the addition of nutrients to stimulate phytoplankton growth to final concentrations of 17 µmol l⁻¹ NO₃⁻ and 1.0 µmol l⁻¹ PO₄³⁻ (Hopkins *et al.*, 2010). Throughout the experiment, the enclosure covers were only removed for sampling and the headspaces were flushed with air (ambient conditions) or CO₂-enriched air (750 ppmV, acidified treatment) to help maintain

pH. Seawater samples were collected daily from the mesocosms at 0900 hours and transported to the shoreside laboratory for immediate processing. A total of 5 l of seawater from each mesocosm was filtered through 90 mm diameter Whatman GFF filters (pore size ~0.7 µm) and the material collected on the filters preserved with RNALater (Applied Biosystems/Ambion, Warrington, UK) and stored at -20 °C overnight and then at -80 °C.

DNA extraction and purification

RNALater (Applied Biosystems/Ambion) was removed from thawed subsamples of the filtered material by brief (~20 s) pulse centrifugation in a microcentrifuge. The filters were immersed in 10 mM TrisHCl (pH 8.0), 1 mM EDTA made to 1% w:v SDS and 0.6–3 U ml⁻¹ proteinase K and incubated at 56 °C for 30 min before DNA purification with cetyl trimethyl ammonium bromide, followed by phenol extraction (Ausubel *et al.*, 2002). Following a final extraction with chloroform:isoamyl alcohol (24:1), DNA was ethanol precipitated from the aqueous phase in the presence of glycogen as a carrier and either used directly or further purified using the DNeasy Tissue kit (Qiagen Ltd, Crawley, UK), following the manufacturers instructions.

Chlorophyll extraction

Pigments were extracted in 90% aqueous acetone from subsamples of the filters (corresponding to a filtered volume of 0.2381 l), and chlorophyll_a concentrations determined spectrophotometrically, using the trichromatic equations of Jeffrey and Humphrey (1975).

*Amplification of form I *rbcL* by the PCR*

Degenerate Form I primers were designed using an alignment of more than 3000 RbcL sequences, including all four major forms of the enzyme (Forms IA–ID), downloaded from the NCBI GenBank database. The forward primer (Table 1) targets the conserved domain KDDEN(I/V)N that forms part of the RubisCO active site, whereas the reverse primer targets the highly conserved motif VVGKLEG (Xu and Tabita, 1996) corresponding to residues 201–207 and 331–337, respectively, of RbcL from *Micromonas pusilla* strain RCC299 (GenBank accession ACO55540). The primers were tested with DNA extracted from *Synechococcus* sp. strain WH8103 (Form IA), *M. pusilla*, *Synechococcus* sp strain PCC7002, (both Form IB), *Rhodobacter sphaeroides* (Form IC), *Emiliania huxleyi*, *Coccolithus pelagicus*, *Thalassiosira pseudonana* (all Form ID) and a PCR product of the expected size was obtained from each.

In the context of the present study, the priming sites targeted are present in the 17 *Micromonas* RbcL sequences reported by Slapeta *et al.* (2006), whereas the only *Bathycoccus* RbcL sequence in the

Table 1 Oligonucleotide primers developed and used in this study

Primer	DNA sequence (5'–3')	Product size (bp)
Form I forward	AARGAYGAYGARAACRTHAAC	411
Form I reverse	CCTTCNARYTTDCCNACNAC	411
Form IB forward	GARGAAGGNTCNGTNACNAA	597
Form IB reverse	TGRTTWCKTTGACGRCAAT	597
BathyIB forward	AACGCTACAGCTGCAMACGT	218
MicroIB forward	AACGTAAGTGCWGTACATC	218
PrasinolB reverse	ACACGGAAGTGAATACCGTG	218

databases has a very rare substitution (KDDEDVN) in the forward primer target sequence (the reverse priming site is present), which results in a single nucleotide mismatch to the forward primer. This reference sequence (Accession number BPU30275) has a number of uncalled bases in the nucleotide sequence and, with a single unrelated exception, a match to the forward priming site (KDDENVN) was found in more than 20 independent *Bathycoccus*-like clones obtained in this study, using the Form IB *rbcl*-specific primers described below.

The Form IB primers target the motifs EEGSVTN and IDRQRNH (Table 1) corresponding to residues 109–115 and 301–307, respectively, of *RbcL* from *M. pusilla* strain RCC299. The forward primer is a match for *Bathycoccus* and the 17 *Micromonas* reference sequences (Slapeta *et al.*, 2006), whereas the reverse primer has two mismatches to these target sequences located at position –12, relative to the priming site, and at a second position further towards the 5'-end of the primer. The primers were tested against DNA extracted from *M. pusilla* (and Form IB containing cyanobacteria) and a PCR product of the expected size (597 bp) was successfully amplified.

Form I *rbcl* was amplified from the mesocosm DNA samples obtained from all six enclosures on 3 days using either the Form I primers (days 1 and 7) or the Form IB primers (day 4). The reactions were performed using the ThermoPrime DNA polymerase, as recommended by the supplier (Thermo Fisher Scientific, Loughborough, UK), in 25 µl reactions amended to 0.4 mg ml⁻¹ bovine serum albumin, 2.0 mM (Form IB) or 2.5 mM (Form I) MgCl₂, and containing 50 pmol of each primer and 1 µl DNA (~10–50 ng). After an initial denaturation at 95 °C for 5 min, cycling conditions were 95 °C for 1 min, 47 °C (Form I) or 50 °C (Form IB) for 1 min, 72 °C for 1.5 min for 40 cycles, followed by a final extension at 72 °C for 10 min.

PCR products were run out in 1% agarose gels and purified using the Wizard SV Gel and PCR Clean-Up System (Promega Ltd, Southampton, UK). For each time point, PCR products obtained from each treatment replicate ($n=3$) were pooled and TA cloned in the plasmid vector pCR2.1 (Invitrogen Ltd, Paisley, UK). Recombinant colonies were picked and propagated in terrific broth in 96 well plates, and plasmid DNA purified with the Seq Prep

96 Plasmid Prep Kit (Edge Biosystems, Gaithersburg, MD, USA), according to the manufacturers recommended protocol for high volume cultures. DNA sequencing of both strands was performed at the NERC Biomolecular Analysis Facility at the University of Edinburgh, (Edinburgh, UK) on an ABI 3730 automated sequencer (Applied Biosystems). The GenBank accession numbers of the sequences analysed here are given in Supplementary Figures S1 and S2.

Phylogenetic analysis

Form I *rbcl* sequences were trimmed of primer sequences and the derived peptide sequences of the inserts aligned using ClustalX (Jeanmougin *et al.*, 1998). Phylograms were constructed using TREECON for Windows software based on the distance calculation of Kimura and a neighbour-joining routine to infer tree topology (Van de Peer and De Wachter, 1994). Mesocosm sequences clustering with Form IB RubisCO were identified and consensus Form IB phylogenetic trees based on one thousand bootstrap replicates were constructed, using neighbour-joining and maximum parsimony (protein sequence parsimony method, ProtPars) routines from TREECON and Phylip (Felsenstein, 1989), respectively, and rooted with Form IA RubisCO from *Synechococcus* sp. strain WH5701.

To investigate the diversity within the *Micromonas*-like *rbcl* sequences that we recovered on days 1 and 7, the nucleotide sequences were trimmed of primer sequences and aligned with 17 DNA sequences from cultured representatives of *Micromonas pusilla* (Slapeta *et al.*, 2006). Consensus neighbour-joining trees were constructed (1000 bootstrap replicates) with the TREECON for Windows software package (<http://bioinformatics.psb.ugent.be/software/details/3>), as described and routed using *rbcl* sequences from *Ostreococcus tauri* and *Bathycoccus prasinos*.

Quantitative PCR

Assays were performed to quantify the abundance of specific Form IB *rbcl* sequences in DNA samples obtained from the six mesocosms during the period 6–13 May 2005 (days 0–7). Forward primers (BathyIB forward and MicroIB forward) targeting the two

main groups of prasinophyte sequences (*Bathycoccus*-like and *Micromonas*-like, respectively) detected in this study and a group-specific reverse primer (PrasinoIB reverse) were designed from an alignment of all Form IB *rbcL* sequences recovered from the mesocosms during this experiment (Table 1). The forward and reverse primers target the same internal region corresponding to nucleotides 721–740 and 918–938 in *rbcL* from *M. pusilla* strain RCC299 (GenBank accession number ACO55540).

The BathyIB forward primer has a single mismatch to the only *rbcL* sequence for *B. prasinos* in the GenBank database (accession number BPU30275), whereas the PrasinoIB reverse primer is a 100% match. The MicroIB forward and PrasinoIB reverse primers are either identical to or contain a single mismatch to the targeted region of *rbcL* from the 17 *M. pusilla* strains investigated by Slapeta *et al.* (2006), with the exception of strain CCMP2099 for which six mismatches were found in the forward primer. Although the primers were specifically designed to target the *Bathycoccus*-like and *Micromonas*-like *rbcL* sequences that we recovered from the mesocosm DNA samples (for which they are 100% matches), we would also expect the primers to amplify the targeted region from the majority of these related *rbcL* sequences with reasonable efficiency.

Assays were carried out with Power SYBR Green PCR Mastermix (Applied Biosystems), as recommended by the supplier, on a Stratagene MX3000p QPCR system (Agilent Technologies Ltd, Stockport, UK) in 25 μ l volumes containing 1 μ l of DNA and 25 pmol each of the appropriate primers. Cycling conditions were 95 °C for 15 s, 61 °C for 15 s and 72 °C for 1 min for 40 cycles, with data collection at the end of the extension phase. The presence of a single product for each sample was verified by inspection of the dissociation curves and confirmed by agarose gel electrophoresis.

Linear fragments containing the two *rbcL* target sequences were obtained by EcoRI digestion of plasmids piiC11 and piiA01 (GenBank accession numbers EU977903 and EU977850) and used as standards for assays performed with the BathyIB/PrasinoIB and MicroIB/PrasinoIB primers, respectively. Standard curves were generated using a 10-fold dilution series of each target and PCR efficiency was determined by linear regression analysis of the slope of log copy number against Ct and used to estimate the original number of copies of *rbcL* in each mesocosm DNA sample. PCR efficiency was 103.8% ($r^2 = 0.992$) for the assays performed with BathyIB/PrasinoIB primers and 100.39% ($r^2 = 0.996$) for the MicroIB/PrasinoIB primers. Negative controls contained all reagents and appropriate primers, plus a spike of the non-target *rbcL* fragment ($\sim 10^6$ copies), that is, the *Bathycoccus*-like *rbcL* EcoRI fragment in the assays containing the MicroIB/PrasinoIB primer pair and *Micromonas* fragment for the BathyIB/PrasinoIB primers.

The quality of each DNA sample ($n = 40$) was assessed in reactions containing 1 μ l of sample DNA and a spike of a linear DNA target obtained by amplifying the insert of a pCR2.1 construct harbouring a fragment of *glgA* from *Synechococcus* sp. strain WH8103 (GenBank accession number GU808826) with M13 primers. Quantitative PCR was carried out in 25 μ l reactions, containing 25 pmol each of TOPO*forw* and TOPO*rev* primers that target pCR2.1 vector sequences flanking the insert downstream of the M13 priming sites (Bird *et al.*, 2005). Reaction and cycling conditions were as described above, except that the annealing temperature was reduced to 60 °C. The absence of detectable PCR inhibitors in the samples was confirmed by obtaining a mean Ct (20.14 ± 0.56) that was not significantly higher than that of spiked-control reactions in which sample DNA was replaced with an equal volume of DNA/RNA-free deionised water.

Statistical analysis

Fisher's exact test (<http://www.quantitativeskills.com/sisa/statistics/fisher.htm>) was used to test the evenness of the distribution of *Bathycoccus*-like and *Micromonas*-like sequences in the *rbcL* clone libraries prepared from DNA samples, obtained from the two CO₂ treatments at each time point (days 1, 4 and 7).

Results and discussion

Bloom development

Following the addition of nutrients, mean chlorophyll_a concentrations increased over the first week of the experiment to reach a peak on day 7 in both treatments (Figure 1). Bloom development was somewhat delayed in the acidified mesocosms and

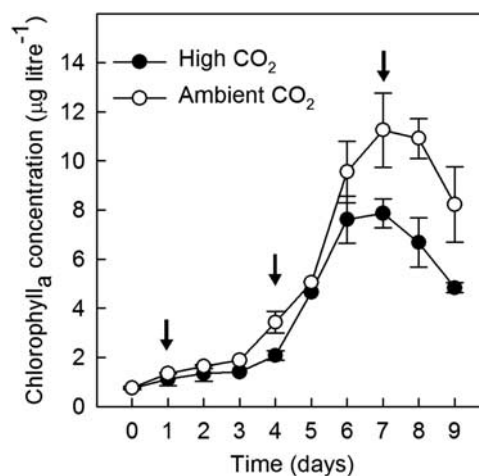


Figure 1 Temporal evolution of mean (\pm s.e., $n = 3$) chlorophyll_a concentrations during the development and initial demise of the phytoplankton blooms in the ambient (open circles) and acidified (closed circles) enclosures.

mean chlorophyll_a concentrations at the peak of the blooms were ~40% higher under ambient CO₂. The phytoplankton populations in both treatments were dominated numerically by picoeukaryotes, whereas cryptophytes, prymnesiophytes (including coccolithophores) and other flagellates of uncertain taxonomic affiliations made the greatest contributions to phytoplankton biomass (Hopkins *et al.*, 2010). Although not identified taxonomically, two size classes of picoeukaryotes ('small' and 'large') were present. The former were found in similar numbers (up to 60 000 cells ml⁻¹) in both treatments, whereas the peak concentration of large picoeukaryotes was somewhat lower and significantly lower under high CO₂ (Hopkins *et al.*, 2010).

The increase in phytoplankton biomass during the first week of the experiment resulted in the progressive drawdown of CO₂ in both treatments, such that pH increased in the acidified mesocosms from 7.8 to 7.83–7.87 on day 4 and further to 8.0 by day 7 (Hopkins *et al.*, 2010). As this study was primarily concerned with the effect of acidification on phytoplankton community composition (and specifically on picoeukaryotes), the observations reported here are confined primarily to the first 7 days of the experiment, when seawater pH in the acidified mesocosms remained between ~0.2–0.4 units lower than ambient.

Diversity of form I *rbcl* sequences

Form I *rbcl* gene libraries were constructed, screened and sequenced on five occasions during the experimental period. Sequences derived from organisms producing the four major forms of RubisCO (Forms IA–ID) were recovered on each occasion. The Form IA sequences were dominated by picocyanobacteria most closely related to the coastal isolate, *Synechococcus* sp. strain CC9902. Their representation in the Form I libraries diminished at the peak of the blooms (Figure 2) before becoming the dominant *rbcl* sequence, recovered from both treatments toward the end of the experiment (data not shown). Prasinophytes dominated the Form IB sequences throughout the development of the blooms, whereas the majority of Form IC genes found during the experiment were identical to or very similar to the Form I gene from the alphaproteobacterium, *Rhodobacter sphaeroides*. A greater diversity of Form ID sequences was encountered including those from members of the Haptophyceae related to *E. huxleyi* and *Phaeocystis pouchetti* commonly recorded in these waters (Egge and Jacobsen, 1997) and an interesting group of sequences related to members of the Chrysophyceae retrieved from the ambient CO₂ treatments only.

With the notable exception of the prasinophyte Form IB sequences, there was little evidence of unevenness in the distribution of *rbcl* phylotypes between treatments for other taxonomic groups. Phylogenetic analysis of the Form IB *rbcl* sequences



Figure 2 Pie charts showing the percentage distribution of Form IA, IB, IC and ID *rbcl* phylotypes recovered from clone libraries prepared from phytoplankton samples collected on day 1 (7 May; top) and day 7 (13 May; bottom) from the ambient (left) or acidified mesocosms (right). The Form IB sequences are further subdivided to show the distribution of *Bathycoccus*-like, *Micromonas*-like and other prasinophyte sequences.

Table 2 One sided *P*-values for $p(O \geq E)$ calculated using Fisher's exact test based on the null hypothesis that there was no unevenness in the distribution of form IB *rbcl* *Micromonas*-like and *Bathycoccus*-like sequences between treatments

Day (Date)	Total number of cases	<i>P</i> -value
1 (7 May)	32	0.760256
4 (10 May)	24	0.000489
7 (13 May)	47	0.000000

recovered on the day following nutrient addition (day 1) showed that phylotypes identical to or very closely related to *Micromonas pusilla* and *Bathycoccus prasinus* were present in both mesocosm treatments (Supplementary Figure S1), whereas at the peak of the bloom, 6 days later, a pronounced skew in their distribution was apparent (Supplementary Figure S2). The form IB sequences recovered from the ambient CO₂ mesocosms clustered almost exclusively with *B. prasinus*, whereas, in marked contrast, those from the acidified mesocosms were predominantly related to *M. pusilla*.

The statistical significance of the observed shift in prasinophyte *rbcl* distribution between treatments was tested using Fisher's exact test for both of these sampling points, and also for an intermediate time point (day 4), using additional frequency data

derived from community analysis of libraries constructed using the Form IB-targeted primer pair (Table 2). The null hypothesis that there was no significant unevenness in the distributions of *rbcl* from the two prasinophyte groups between CO₂ treatments was supported on the first sampling day, whereas *P*-values were <0.001 on both days 4 and 7; that is, the two phlotypes were no longer found to be evenly distributed between treatments in these later samples. The phylogenetic and associated statistical analysis, therefore, strongly suggests that *Micromonas*-like prasinophytes preferred the acidified conditions, whereas *Bathycoccus*-like prasinophytes were more dominant under ambient CO₂ conditions.

To assess whether the clone libraries provided a representative indication of the distribution of *Micromonas*-like and *Bathycoccus*-like phlotypes between treatments, we estimated the concentrations of the *rbcl* genes belonging to each prasinophyte by quantitative PCR in DNA samples taken from the mesocosms between days 0–7 (Figure 3). Similar numbers of copies of the *Bathycoccus*-like *rbcl* were present under high ($7.67 \pm 3.82 \times 10^3$) and low ($5.35 \pm 2.57 \times 10^3$) CO₂ at the start of the experiment on day 0. The concentrations of the *Micromonas*-like sequence were $1.8 \pm 1.27 \times 10^4$ and $0.32 \pm 0.26 \times 10^4$ copies ml⁻¹ under high and low CO₂, respectively, whereas of a similar magnitude to those estimated for the *Bathycoccus*-like *rbcl*, were somewhat higher in the samples taken from the acidified enclosures than under ambient conditions.

The concentrations of *rbcl* from both prasinophytes increased dramatically over the next few days in samples taken from the high CO₂ enclosures (Figure 3). By day 4, *Bathycoccus*-like *rbcl* was present at ~12-fold higher concentrations

($9.27 \pm 3.87 \times 10^4$ copies ml⁻¹) than on day 0, whereas the abundance of the *Micromonas*-like sequence had increased ~13-fold ($2.39 \pm 1.1 \times 10^5$ copies ml⁻¹) to more than twice (~2.6-fold) the concentration of the *Bathycoccus*-like gene in this treatment. A very different response was observed in the ambient enclosures meanwhile (Figure 3). Whereas the concentration of the *Bathycoccus*-like *rbcl* sequence was similar ($8.37 \pm 5.43 \times 10^4$ copies ml⁻¹) to that observed in the acidified enclosures by day 4, the concentration of the *Micromonas*-like sequence ($1.38 \pm 0.4 \times 10^4$ copies ml⁻¹) was only ~four-fold higher than on day 0, some six-fold less abundant than *Bathycoccus*-like *rbcl* in these enclosures and 17-fold less abundant than *Micromonas*-like *rbcl* in the acidified treatment.

Thereafter, little further increase was observed in the concentrations of *Bathycoccus*-like *rbcl* in either treatment (Figure 3), whereas the abundance of *Micromonas*-like *rbcl* declined from the peak observed on day 4 to $1.55 \pm 0.76 \times 10^5$ copies ml⁻¹ in the acidified enclosures by day 7 and to $6.88 \pm 3.08 \times 10^3$ copies ml⁻¹ under ambient conditions. By day 7, therefore, the *Micromonas*-like sequence was present in the ambient CO₂ enclosures at a concentration ~23-fold lower than that found under high CO₂ and ~16-fold lower than the concentration of the *Bathycoccus*-like sequence in these enclosures at this time point ($1.13 \pm 0.32 \times 10^5$ copies ml⁻¹).

In comparison to day 0, when the concentrations of both targets was similar, the pronounced unevenness we observed in the distribution of *Bathycoccus*-like and *Micromonas*-like sequences in the *rbcl* clone libraries prepared from DNA isolated from the mesocosms on days 4 and 7, therefore, was due to (i) the far higher abundance of the *Bathycoccus*-like *rbcl* gene in the ambient enclosures at these time points and (ii) the higher concentrations of *Micromonas*-like sequences compared with *Bathycoccus*-like *rbcl* in the high CO₂ treatment.

In summary, therefore, we observed a consistent and pronounced increase in *Micromonas*-like *rbcl* concentrations in the acidified mesocosms over the first four days of the experiment that was not observed under ambient conditions. Significantly, this occurred during the initial phase of the experiment when pH within the acidified mesocosms was close to that at the start of the experiment (pH 7.8) and this trend was not maintained after day 4, once the pH began to increase (Hopkins *et al.*, 2010).

Because of the polyploid nature of the chloroplast genomes of algae and green plants (Maguire *et al.*, 1995; Koumandou and Howe, 2007), it is not possible to directly relate the changes in prasinophyte *rbcl* concentrations that we observed to changes in the population sizes of the two prasinophyte groups within the mesocosms. However, for *Micromonas*, at least, we were able to approximate

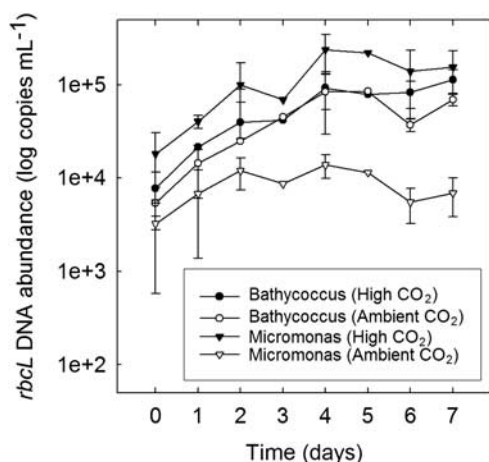


Figure 3 Temporal variability in log mean (\pm s.e., $n=3$) *Bathycoccus*-like and *Micromonas*-like *rbcl* copies ml⁻¹ determined by quantitative PCR between the start of the experiment on day 0 and the observed peaks in chlorophyll concentrations on day 7. The data presented are biological replicates from the two treatments with the exception of days 3 and 5 on which only mesocosm 2 (high CO₂) and 5 (ambient CO₂) were sampled.

the possible scale of the increase in cell numbers in the two treatments, using previously published data. Brown *et al.* (2007) showed that *rbcL* was present at approximately the same number of copies per cell as 18S rRNA in *M. pusilla* CCMP491, which has been estimated to be five copies per cell in the closely related strain CCMP490 (Zhu *et al.*, 2005). If a similar number of *rbcL* copies per cell was maintained in the *Micromonas* population we sampled, this would translate to an increase from an initial mean population size on day 0 of 640 to 2760 cells ml⁻¹ on day 4 under ambient conditions, and from 3600 cells ml⁻¹ to 47 800 cells ml⁻¹ in the acidified mesocosms over the same period. Although these estimates are speculative, we note that they are not too dissimilar to the concentrations of small picoeukaryotes reported by Hopkins *et al.* (2010) that, we presume, included *Micromonas* and *Bathycoccus*. They recorded cell counts of ~30 000 cells ml⁻¹ on day 4 rising to peaks of 40 000–55 000 cells ml⁻¹ on day 5 in the acidified mesocosms, whereas the abundance of small picoeukaryotes was lower between these days at 13 000–20 000 cells ml⁻¹ in the control mesocosms in which the peak in population size was not reached until day 8 (Hopkins *et al.*, 2010).

It has been proposed that phytoplankton that lack an efficient carbon concentrating mechanism (CCM) might be favored in a high CO₂ world (Engel *et al.*, 2008). The CO₂ limitation of diatom growth has been shown in some species (Riebesell *et al.*, 1993), but not others (Goldman, 1999), whereas carbon fixation by *E. huxleyi* has been shown to be limited at current atmospheric CO₂ concentrations (Rost and Riebesell, 2004; Riebesell *et al.*, 2007). Phytoplankton growth is generally regarded to be CO₂-saturated in the modern ocean, however (The Royal Society, 2005), and the small size of eukaryotic picoplankton would appear to militate against CO₂ limitation as the explanation for the positive response of *Micromonas*-like prasinophytes to high CO₂/acidification reported here (Raven, 1991).

A highly efficient CCM has been demonstrated experimentally in *M. pusilla* strain PCC No. 27 (PLY27), but this was induced only at CO₂ concentrations well below current levels (Iglesias-Rodríguez *et al.*, 1998). Induction was accompanied by the development of extracellular carbonic anhydrase activity, and several genes encoding carbonic anhydrase are present in the genomes of *M. pusilla* strains CCMP1545 (synonym PLY27) and RCC299. Furthermore, extensive genomic analysis of these *M. pusilla* strains revealed the presence of not one, but two distinct types of CCM in both strains (Worden *et al.*, 2009). By contrast to *Bathycoccus*, however, several genetic lineages of *Micromonas* have been described (for example, Guillou *et al.*, 2004; Slapeta *et al.*, 2006) and individual strains may have divergent capacities to operate CCMs. The *Micromonas*-like *rbcL* phylotypes that we recovered from both CO₂ treatments on days 1 and 7 shared

99–100% identity at the nucleotide level to *M. pusilla* strain NEPCC29, 98–99% to strains CS222 and CCMP1195 and between 91–96% nucleotide identity to the *rbcL* genes of the remaining 14 strains of *M. pusilla* sequenced by Slapeta *et al.*, (2006). Phylogenetic analysis revealed that all of the *Micromonas*-like *rbcL* phylotypes present on both days and in both treatments clustered within *M. pusilla* lineage C that includes strains NEPCC29, CS222 and CCMP1195 (Supplementary Figures S3 and S4), whereas in agreement with the much more extensive analysis reported by Slapeta *et al.* (2006), one of the sequenced strains (CCMP1545) was found in a separate lineage that they designate lineage D. The *rbcL* gene of *M. pusilla* strain RCC299 was not included in the Slapeta *et al.* (2006) study, but a BLAST search of the GenBank database reveals that it shares 100% nucleotide identity to a member of lineage A (strain MPIC10095) over the region we analysed, a finding that is consistent with analysis of 18S rRNA genes from these two strains in which both were placed in the same lineage (designated MII) by Worden *et al.* (2009).

We are aware of one other study in which pCO₂ perturbations have been shown to impact on the development of the picoeukaryote community (Engel *et al.*, 2008). On the basis of the flow cytometric analysis and confirmed by microscopy, these authors report that *Micromonas*-like cells were less abundant in blooms under past atmospheric conditions (190 ppmV CO₂) than under either present day and, in particular, future (700 ppmV) conditions. Engel *et al.* (2008) interpret these observations as evidence for the failure of *Micromonas* to operate CCMs efficiently at ambient (and past) CO₂ concentrations.

The findings reported here are certainly consistent with this interpretation. The operation of CCMs is energetically expensive and, because cell membranes are freely permeable to CO₂, additional metabolic costs are incurred in limiting the efflux of CO₂ from the cell (Giordano *et al.*, 2005). It may be that the energetic savings made by downregulating CCMs are significant under elevated CO₂ in at least some strains of *Micromonas*, therefore, although these benefits may be offset to some degree by the increased costs of other metabolic processes (Raven and Johnston, 1991).

In addition to the possible relief of CO₂ limitation, acidification may influence the distribution of potential predators of individual phytoplankton species. Acidification has been shown to reduce viral production in mixed blooms dominated by diatoms and *E. huxleyi* (Larsen *et al.*, 2008), for example, although little effect was found on microzooplankton standing stock or grazing activity (Suffrian *et al.*, 2008). *M. pusilla* populations can collapse rapidly due to viral lysis and microzooplankton grazing (Evans *et al.*, 2003), and it is possible that the shifts in picoeukaryote community composition we observed in the present study may

have been due to reduced predation of *Micromonas* in the acidified enclosures. Future work should examine the effects of acidification on predator prey dynamics within picoeukaryote communities, therefore, as well as focus on the CCMs of different strains of *M. pusilla* and their sensitivities to $p\text{CO}_2$ and nutrient availability.

Because of the complexity of marine ecosystems, extrapolating the outcomes of $p\text{CO}_2$ perturbation experiments to predictions of how acidification will impact on specific groups of organisms over longer time scales needs to be undertaken with extreme caution (The Royal Society, 2005). Our findings show that acidification has at least the potential to promote the growth of the picoeukaryote *Micromonas*, whereas others like *Bathycoccus* appear to be insensitive to short-term changes in seawater pH/ $p\text{CO}_2$.

Acknowledgements

This research was supported by the Natural Environment Research Council Post-Genomics and Proteomics Programme: Ref. NE/C507902/1 and a NERC studentship awarded to NM. We are grateful to Dr Rachel M Jones for her contributions to the field work and the purification of DNA samples, and to Dr Ian Joint and the other scientists who participated in the Bergen mesocosm study for their help and assistance.

References

- Ausubel FM, Brent R, Kingston RE, Moore DD, Seidman JG, Smith JA *et al.* (2002). *Short Protocols in Molecular Biology*. Wiley: New York.
- Bird C, Martinez Martinez J, O'Donnell AG, Wyman M. (2005). Spatial distribution and transcriptional activity of an uncultured clade of planktonic diazotrophic gamma-proteobacteria in the Arabian Sea. *Appl Environ Microbiol* **71**: 2079–2085.
- Breitbarth E, Bellerby RJ, Neill CC, Ardelan MV, Meyerhofer M, Zollner E *et al.* (2010). Ocean acidification affects iron speciation during a coastal seawater mesocosm experiment. *Biogeosciences* **7**: 1065–1073.
- Brown CM, Douglas DA, Lawrence JE. (2007). Resource dynamics during infection of *Micromonas pusilla* by virus MpV-Sp1. *Env Microbiol* **9**: 2720–2727.
- Caldiera K, Wickett ME. (2003). Anthropogenic carbon and ocean pH. *Nature* **425**: 365.
- Doney SC, Fabry VJ, Feely RA, Kleypas JA. (2009). Ocean acidification: the other CO_2 problem. *Annu Rev Mar Sci* **1**: 169–192.
- EGge JK, Jacobsen A. (1997). Influence of silicate on particulate carbon production in phytoplankton. *Mar Ecol Prog Ser* **147**: 219–230.
- Engel A, Schulz KG, Riebesell U, Bellerby R, Delille B, Schartau M. (2008). Effects of CO_2 on particle size distribution and phytoplankton abundance during a mesocosm bloom experiment (PeECE II). *Biogeosciences* **5**: 509–521.
- Evans C, Archer SD, Jacquet S, Wilson WH. (2003). Direct estimates of the contribution of viral lysis and microzooplankton grazing to the decline of a *Micromonas* spp. population. *Aquat Microb Ecol* **30**: 207–219.
- Fabry VJ, Siebel BA, Feely RA, Orr JC. (2008). Impacts of ocean acidification on marine fauna and ecosystem processes. *ICES J Mar Sci* **65**: 414–432.
- Felsenstein J. (1989). PHYLIP: phylogeny inference package (Version 3.2). *Cladistics* **5**: 164–166.
- Giordano M, Beardall J, Raven JA. (2005). CO_2 concentrating mechanisms in algae: mechanism, environmental modulation, and evolution. *Annu Rev Plant Biol* **56**: 99–131.
- Goldman JC. (1999). Inorganic carbon availability and the growth of large marine diatoms. *Mar Ecol Prog Ser* **180**: 81–91.
- Guillou L, Eikrem W, Chrétiennot-Dinet M-J, Le Gall F, Massana R, Romari K *et al.* (2004). Diversity of picoplanktonic prasinophytes assessed by direct nuclear SSU rDNA sequencing of environmental samples and novel isolates retrieved from oceanic and coastal marine ecosystems. *Protist* **155**: 193–214.
- Guinotte JM, Fabry VJ. (2008). Ocean acidification and its potential effects on marine ecosystems. *Ann NY Acad Sci* **1134**: 320–342.
- Hopkins FE, Turner SM, Nightingale PD, Steinke M, Bakker D, Liss PS. (2010). Ocean acidification and marine trace gas emissions. *Proc Natl Acad Sci USA* **107**: 760–765.
- Iglesias-Rodríguez MD, Nimer NA, Merrett MJ. (1998). Carbon dioxide-concentrating mechanism and the development of extracellular carbonic anhydrase in the marine picoeukaryote *Micromonas pusilla*. *New Phytol* **140**: 685–690.
- Jeanmougin F, Thompson JD, Gouy M, Higgins DG, Gibson TJ. (1998). Multiple sequence alignment with Clustal X. *Trends Biochem Sci* **23**: 403–405.
- Jeffrey SW, Humphrey GF. (1975). New spectrophotometric equations for determining chlorophylls *a*, *b*, *c*₁ and *c*₂ in higher plants, algae and natural phytoplankton. *Biochem Physiol Pflanz* **167**: 191–194.
- Koumandou VL, Howe CJ. (2007). The copy number of chloroplast gene minicircles changes dramatically with growth phase in the dinoflagellate *Amphidinium operculatum*. *Protist* **158**: 89–103.
- Larsen JB, Larsen A, Thyrrhaug R, Bratbak G, Sandaa R-A. (2008). Response of marine viral populations to a nutrient induced phytoplankton bloom at different $p\text{CO}_2$ levels. *Biogeosciences* **5**: 523–533.
- Li WKW. (1994). Primary production of prochlorophytes, cyanobacteria, and eukaryotic ultraplankton: measurements from flow cytometric cell sorting. *Limnol Oceanogr* **39**: 169–175.
- Maguire MJ, Goff LJ, Coleman AW. (1995). *In situ* plastid and mitochondrial DNA determination; implication of the observed minimal plastid genomenuber. *American J Bot* **82**: 1496–1506.
- Marie D, Zhu F, Balagué V, Ras J, Vaultot D. (2006). Eukaryotic picoplankton communities of the Mediterranean Sea in summer assessed by molecular approaches (DGGE, TTGE, QPCR). *FEMS Microbiol Lett* **55**: 403–415.
- Moon-van der Staay SY, De Wachter R, Vaultot D. (2001). Oceanic 18S rDNA sequences from picoplankton reveal unsuspected eukaryotic diversity. *Nature* **409**: 607–610.
- Not F, Latasa M, Marie D, Cariou T, Vaultot D, Simon N. (2004). A single species, *Micromonas pusilla* (Prasinophyceae), dominates the eukaryotic picoplankton in

- the Western English Channel. *Appl Environ Microbiol* **70**: 4064–4072.
- Raven JA. (1991). Implications of inorganic carbon utilization: ecology, evolution and geochemistry. *Can J Bot* **69**: 908–924.
- Raven JA, Johnston AM. (1991). Mechanisms of inorganic-carbon acquisition in marine phytoplankton and their implications for the use of other resources. *Limnol Oceanogr* **36**: 1701–1714.
- Riebesell U, Schulz KG, Bellerby RGJ, Botros M, Fritsche P, Meyerhöfer M *et al.* (2007). Enhanced biological carbon consumption in a high CO₂ ocean. *Nature* **450**: 545–549.
- Riebesell U, Wolf-Gladrow D, Smetacek V. (1993). Carbon dioxide limitation of marine phytoplankton growth rates. *Nature* **361**: 249–251.
- Rost B, Riebesell U. (2004). Coccolithophores and the biological pump: responses to environmental changes. In: Thierstein HR, Young JR (eds). *Coccolithophores—From Molecular Processes to Global Impact*. Springer: New York, pp 99–125.
- Slapeta J, Lopez-Garcia P, Moriera D. (2006). Global dispersal and ancient cryptic species in the smallest eukaryotes. *Mol Biol Evol* **23**: 23–29.
- Suffrian K, Simonelli P, Nejstgaard JC, Putzeys S, Carotenuto Y, Antia AN. (2008). Microzooplankton grazing and phytoplankton growth in marine mesocosms with increased CO₂ levels. *Biogeosciences* **5**: 1145–1156.
- Stockner JG. (1988). Phototrophic picoplankton: an overview from marine and freshwater ecosystems. *Limnol Oceanogr* **33**: 765–775.
- The Royal Society (2005). Ocean acidification due to increasing atmospheric carbon dioxide. Policy Document 12/05. *Roy. Soc. Rep.* 12: Royal Society: London.
- Van de Peer Y, De Wachter R. (1994). TREECON for Windows: a software package for the construction and drawing of evolutionary trees for the Microsoft Windows environment. *Comput Applic Biosci* **10**: 569–570.
- Vaulot D, Eikrem W, Viprey M, Moreau H. (2008). The diversity of small eukaryotic phytoplankton ($\leq 3\ \mu\text{m}$) in marine ecosystems. *FEMS Microbiol Rev* **32**: 795–820.
- Worden AZ. (2006). Picoeukaryote diversity in coastal waters of the Pacific Ocean. *Aquat Microb Ecol* **43**: 165–175.
- Worden AZ, Lee J-H, Mock T, Rouze P, Simmons MP, Aerts AL *et al.* (2009). Green evolution and dynamic adaptations revealed by genomes of the marine picoeukaryotes *Micromonas*. *Science* **324**: 268–272.
- Worden AZ, Nolan JK, Palenik B. (2004). Assessing the dynamics of marine picophytoplankton: the importance of the eukaryotic component. *Limnol Oceanogr* **49**: 168–179.
- Xu HH, Tabita FR. (1996). Ribulose-1,5-bisphosphate carboxylase/oxygenase gene expression and diversity of Lake Erie planktonic microorganisms. *Appl Environ Microbiol* **62**: 1913–1921.
- Zhu F, Massana R, Not F, Marie D, Vaulot D. (2005). Mapping of picoeukaryotes in marine ecosystems with quantitative PCR of the 18S rRNA gene. *FEMS Microbiol Lett* **52**: 79–92.

Supplementary Information accompanies the paper on The ISME Journal website (<http://www.nature.com/ismej>)